Acta Pharmacologica Sinica 2017: 1150–1160
 1671-4083/17
www.nature.com/aps

Original Article

Plumbagin suppresses chronic periodontitis in rats via down-regulation of TNF-α, IL-1β and IL-6 expression

Xin-yi ZHENG[1,2], Chuan-yuan MAO[2], Han QIAO[3], Xi ZHANG[2], Li YU[1,*], Ting-yu WANG[4,*], Er-yi LU[1,*]

[1]Department of Stomatology, Renji Hospital, School of Medicine, Shanghai JiaoTong University, Shanghai 200127, China; [2]College of Stomatology, Shanghai JiaoTong University School of Medicine, Shanghai 200025, China; [3]Shanghai Key Laboratory of Orthopedic Implant, Department of Orthopedic Surgery, Shanghai Ninth People's Hospital, Shanghai JiaoTong University School of Medicine, Shanghai 200011, China; [4]Department of Pharmacy, Shanghai Ninth People's Hospital, Shanghai JiaoTong University School of Medicine, Shanghai 200011, China

Abstract

Chronic periodontitis (CP) is one of the most common oral diseases, which causes alveolar bone absorption and tooth loss in adults. In this study we aimed to investigate the potential of plumbagin (PL), a widely-investigated active compound extracted from the traditional Chinese herb *Plumbago zeylanica* L in treating CP. Human periodontal ligament stem cells (PDLSCs) were used for *in vitro* studies, whereas an animal model of CP was established in SD rats by ligation+*Porphyromonas gingivalis* (Pg) stimulation. The rats were injected with PL (2, 4, and 6 $mg \cdot kg^{-1} \cdot d^{-1}$, ip) for 4 weeks. Treatment of PDLSCs with TNF-α (10 ng/mL) markedly stimulated the expression of the proinflammatory cytokines TNF-α, IL-1β and IL-6, as well as the chemokines CCL-2 and CCL-5, which were dose-dependently suppressed by co-treatment with PL (1.25–5 μmol/L). Furthermore, PL (3.75 μmol/L) markedly suppressed TNF-α-induced activation of the MAPK, NF-κB and JAK/STAT signaling pathways in PDLSCs. In consistence with the *in vitro* studies, PL administration significantly decreased the expression of TNF-α, IL-1β and IL-6 in gingiva of the rat with CP, with the dosage 4 $mg \cdot kg^{-1} \cdot d^{-1}$ showing the best anti-inflammatory effect. Moreover, PL administration decelerated bone destruction in the rat with CP, evidenced by the aveolar bone loss (ABL) and H&E staining results. In conclusion, PL suppresses CP progression in rats by downregulating the expressions of TNF-α, IL-1β and IL-6 and inhibiting the MAPK, NF-κB and JAK/STAT signaling pathways.

Keywords: plumbagin; traditional Chinese herb; chronic periodontitis; periodontal ligament stem cells; TNF-α; IL-1β; IL-6; MAPK; NF-κB; JAK/STAT

Acta Pharmacologica Sinica (2017) 38: 1150–1160; doi: 10.1038/aps.2017.19; published online 29 May 2017

Introduction

Chronic periodontitis (CP), one of the most common oral diseases worldwide, is a long-term infectious disease that leads to inflammation in periodontal tissue, including gingiva, periodontal ligament, cementum and alveolar bone[1]. The colonization of bacterial plaque initiates the pathogenesis of CP, thus resulting in the destruction of connective tissues and alveolar bone and eventually contributing to tooth loss. The main pathogens are anaerobes, such as *Porphyromonas gingivalis*, *Prevotella intermedia*, *Fusobacterium nudeatum* and *Peptostreptococcus anaerobius*, and facultative anaerobes, including *Staphylococcus aureus* and *Staphylococcus epidermidis*[2]. Treatments for CP have highlighted mechanical strategies involving nonsurgical scaling plus root planning (SRP) and drug therapy, which is adjunctive to SRP[3]. However, reliance on antibiotics has significantly limited drug therapy, particularly the use of amoxicillin, metronidazole and ornidazole[4].

Antibiotics have been effective in treating bacterial infections. However, over-dosage or long-term use of antibiotics may lead to antibiotic resistance. To address this issue, traditional Chinese medicine (TCM) has gradually been used as a substitute therapy with minimal relatively mild side effects. Houttuynia cordata has been shown to prevent oral infectious diseases[5]. Gynostemma pentaphyllum and total glucosides of paeony have been used as treatments for oral lichen planus[6]. However, TCMs for treating periodontitis

*To whom correspondence should be addressed.
E-mail lueryi222@outlook.com (Er-yi LU);
drtywang@163.com (Ting-yu WANG);
yuli_renji@163.com (Li YU)
Received 2016-10-29 Accepted 2017-03-13

remain limited. Here, Plumbagin (PL) was found to show potent effects against inflammatory diseases, immunologically mediated diseases, cardiac diseases, and cancer and thus may have potential in treating periodontal disease.

Plumbagin (5-hydroxy-2-methyl-1,4-naphthoquinone), extracted from the roots of *Plumbago zeylanica* L, is used in treating various diseases, such as acne, fractures, and bacterial infections, especially bone diseases[7,8], and it has anti-oxidant, anti-inflammatory, anti-cancerous, anti-bacterial and anti-fungal effects[9]. Among these, the anti-inflammatory properties of PL have been exploited in treating different diseases. Luo has suggested that PL effectively decreases the expression of the pro-inflammatory cytokines interleukin 1 (IL-1), interleukin 6 (IL-6), and tumor necrosis factor alpha (TNF-α) through the inhibition of the NF-κB signaling pathway[10]. Chu has reported that plumbagin significantly inhibits NF-κB expression and upregulates Nrf-2 expression[11]. Shuai has reported that PL protects against glucocorticoid-induced osteoporosis through the Nrf-2 pathway[12]. Bhattacharya has found that PL inhibits cytokinesis in Bacillus subtilis, thereby having antibacterial activity[13]. Wang has suggested that Plumbagin exerts its anti-inflammatory properties by decreasing the expression of cytokines, such as MCP-1, IL-6, IL-8, and TNF-α[14].

Previously, we have found that PL inhibits LPS-induced inflammation through the NF-κB and MAPK pathways[15]. The invasion and migration of breast cancer cells are inhibited by PL through STAT3; there are significant decreases in the mRNA expression levels of IL-1α, TGF-β, MMP-2 and MMP-9[16,17].

We sought to investigate the potential of PL in treating CP. Human periodontal ligament stem cells (PDLSCs) and SD rat models were adopted for *in vitro* and *in vivo* studies. According to the pathogeny of CP, which is based on a combination of bacterial infection and mechanical irritation, the SD rat model was ligated with silk sutures soaked in *Porphyromonas gingivalis* (Pg) to simulate the process of CP. TNF-α, one of the main products of CP inflammation, was used to mimic an inflammatory microenvironment at the periodontitis level in the *in vivo* experiments[19,20]. Ornidazole (OZ) was used as a positive control drug in the *in vitro* experiments.

Materials and methods

Main reagents

Plumbagin (PL), Ornidazole (OZ), dimethyl sulfoxide (DMSO), ampicillin and PEG 3350 were purchased from Sigma-Aldrich (St Louis, MO, USA). TNF-α was purchased from Peprotech (Rocky Hill, NJ, USA). Porphyromonas gingivalis (Pg) was supplied by the Shanghai Research Institute of Stomatology and Shanghai Key Laboratory of Stomatology, Ninth People's hospital, Shanghai Jiao Tong University School of Medicine (Shanghai, China). In the cell experiments, PL was dissolved in DMSO at 100 mmol/L and stored in a dark-colored bottle at -20 °C. For the animal experiments, PL was dissolved in 25% PEG 3350 at 2 mg/mL. Pg was resuspended at 1×10^{10} cells/mL in PBS before use.

Cell preparation and culture

Human periodontal ligament stem cells (PDLSCs) were cultured for the *in vitro* study. PDLSCs have mesenchymal stem cell characteristics with clonogenicity and high proliferation[21]. These cells have the potential to reconstruct tissues destroyed by periodontal diseases and have demonstrated the ability to generate a cementum/PDL-like structure necessary for periodontal tissue repair[22].

Extracted, disease-free premolars were collected from patients. The extracted premolars were preserved in α-modified Eagle's minimum essential medium (α-MEM, HyClone, Logan, UT, USA) and were taken to the laboratory immediately after extraction. Premolars were rinsed with PBS several times before collection of periodontal tissue. The PDL tissue was gently scraped from the surface of the middle one-third of the root and placed into 5-cm culture dishes. Cells were cultured with α-MEM containing 10% fetal bovine serum (FBS, Gibco, Invitrogen Ltd, Carlsbad, CA, USA) and 1% penicillin/streptomycin (Gibco-BRL, Gaithersburg, MD, USA) at 37 °C in a humidified 5% CO_2 atmosphere. PDLSCs were isolated from PDLCs through the limiting dilution method and single-colony selection[23]. Flow cytometry analysis was used to characterize PDLSCs on the basis of surface molecule expression. PDLSCs express mesenchymal surface markers STRO-1, CD146 and CD90, and negatively express endothelial cell marker CD31 and hematopoietic markers CD45 and CD14, as previously reported[24].

Animals

Forty 3-month-old female Sprague-Dawley (SD) rats (300±50 g) were obtained and were raised in the Department of Laboratory Animal Science at Shanghai Ninth People's hospital. The SD rats received 2 weeks acclimatization and were kept in filter-top cages (3 per cage) under a 12-h light-dark cycle. Ampicillin was dissolved in drinking water and given to rats at 20 mg per day per rat 3 days before ligation. These rats were divided into five groups, with 8 per group: (1) control group; (2) chronic periodontitis group (ligation+Pg); (3) PL low-dose group (ligation+Pg+PL 2 mg/kg); (4) PL medium-dose group (ligation+Pg+PL 4 mg/kg); and (5) PL high-dose group (ligation+Pg+PL 6 mg/kg). For groups (2) to (5), the rats were anesthetized with 10% chloralhydrate (4 mL/kg, by intraperitoneal injection) and ligated with silk sutures (3/0) (Johnson & Johnson Medical [China] Ltd, Shanghai, China) into the subgingival of the first and second molars (M1 and M2, respectively) with a continuous "∞" method randomly on one side of the maxilla bone. The sutures were soaked in Pg solution before the surgery. The rats were fed with high-sugar drinking water for 4 weeks. During this period, the ligation was checked twice weekly and was replaced if had been displaced or loosened. Four weeks later, the ligation was removed, and PL was injected intraperitoneally 5 times per week for 4 weeks according to different dosages.

Cell viability assay

Cell viability was assessed using a Cell Counting Kit-8 assay

(CCK-8, Dojindo Laboratories, Kumamoto, Japan). PDLSCs were seeded in a 96-well plate at 5000 cells per well for 24 h. The cells were then treated with different concentrations of PL, OZ and TNF-α for either 24 h or 48 h. Absorbances were measured at 450 nm (630 nm as reference) on a Bio-Tek Synergy HT spectrophotometer. The number of cells counted/*OD* value in the control group was set to 1, and the numbers of cells in the remaining groups were calculated relative to the control group. Each experiment was repeated 3 times.

Real-time PCR on human PDLSCs

Total ribonucleic acid (RNA) was extracted using a Qiagen RNeasy Mini Kit (Qiagen, Valencia, CA, USA). A reverse transcriptase (TaKaRa Biotechnology, Otsu, Japan) was used to synthesize complementary deoxyribonucleic acid (cDNA). Real-time polymerase chain reaction (PCR) was performed using a SYBR® Premix Ex Taq™ Kit (TaKaRa, Otsu, Japan) and an Applied Bio-systems 7500 real-time PCR System.

PDLSCs were seeded in 6-well plates for 24 h. The cells were treated with 10 ng/mL of TNF-α and different concentrations of PL (0, 1.25, 2.5, 3.75 and 5 μmol/L) and OZ (5 and 10 μg/mL) for another 24 h. Real-time PCR reactions were performed in triplicate using the following cycling parameters: initial denaturation at 95 °C for 30 s, 40 cycles of denaturation at 95 °C for 5 s, and annealing at 60 °C for 34 s. The sequences for the relevant primers are listed in Table 1. The expression levels were normalized to that of β-actin. All data were calculated using the $2^{\Delta\Delta Ct}$ method. Each experiment was repeated 3 times.

ELISA

Cell supernatant was collected from the treated PDLSCs. Levels of TNF-α, IL-1β and IL-6 were measured with enzyme-linked immunosorbent assay (ELISA) kits (R&D Systems ValukineTM ELISA) according to manufacturer's instructions. TNF-α was diluted 10 times. Each experiment was repeated 3 times.

Western blotting

Different reaction durations and concentrations were individually tested. PDLSCs were seeded in 6-well plates for 24 h. For the duration test, 3.75 μmol/L PL and 10 ng/mL TNF-α were cultured for 0, 1, 2, 4, 6 and 24 h. For the concentration test, the cells were treated with 10 ng/mL TNF-α and different concentrations of PL (0, 2.5, 3.75 and 5 μmol/L) and OZ (10 μg/mL) for 24 h. The cells were then lysed with RIPA buffer (Beyotime, Shanghai, China) to extract proteins. Protein extracts were separated using SDS-PAGE and transferred to polyvinylidene difluoride membranes (PVDF Millipore, Bedford, MA, USA). The membranes were incubated with primary antibodies (Cell Signaling Technology, Danvers, MA, USA) at 4 °C overnight and subsequently with secondary antibodies Abcam (Cambridge, UK) for 2 h at room temperature. The results were detected with an Odyssey V3.0 image scanner (Li-COR Inc, Lincoln, NE, USA). Each experiment was repeated 3 times.

Table 1. Primer sequences for real-time PCR analysis.

Gene	Forward primer (5'–3')	Reverse primer (5'–3')
β-Actin	TGGCACCCAGCACAATGAA	CTAAGTCATAGTCCGCCTAGAAGCA
TNF-α	CCCATGTTGTAGCAAACCCTC	TATCTCTCAGCTCCACGCCA
IL-1β	CCACCTCCAGGGACAGGATA	TGGGATCTACACTCTCCAGC
IL-6	CAATGAGGAGACTTGCCTGG	TGGGTCAGGGGTGGTTATTG
CCL-2	CGCTCAGCCAGATGCAATCAAT	CTTCTTTGGGACACTTGCTGC
CCL-5	CAGTCGTCCACAGGTCAAGG	CTTGTTCAGCCGGGAGTCAT

Animal tissue collection and maxilla bone analysis

After 4 weeks of model establishment and 4 weeks of drug administration, both sides of the SD rat maxilla were collected and fixed in 4% paraformaldehyde. The gingiva of the SD rat maxilla was removed from bone and stored at -80 °C before RNA extraction.

The ligated sides of the maxilla bone were scanned using a high-resolution μCT scanner (μCT 80; SCANCO Medical AG, Bassersdorf, Switzerland) at an isometric resolution of 10 mm and X-ray energy settings of 70 kV, 114 mA and 8 W. Scans were reconstructed to generate three-dimensional models. Microstructure indicators of bone volume/tissue volume (BV/TV), trabecular thickness (Tb.Th), trabecular separation (Tb.Sp) and trabecular number (Tb.N) were determined using a three-dimensional region of interest (ROI).

Alveolar bone loss (ABL), i.e., the linear distance of the cemento-enamel junction (CEJ) to the alveolar bone crest (ABC), was measured at four points on each tooth, i.e., the first maxillary molar (M1) and the second maxillary molar (M2), which were the mesiolingual (ML), mesiobuccal (MB), distolingual (DL), and distobuccal (DB) regions, with Mimics software (Materialise NV, Belgium). To improve measurement objectivity, two researchers conducted the examination individually, and averages were calculated.

Real-time PCR on SD rat gingiva

Total RNA was extracted and reverse transcribed into cDNA by following the above procedures. Real-time PCR reactions were performed as mentioned above. The primer sequences of relevant pro-inflammatory cytokines are listed in Table 2. The expression levels were normalized to that of β-actin. All data were calculated using the $2^{\Delta\Delta Ct}$ method. Each experiment was repeated 3 times.

Histological staining

The ligated sides and control group of the maxilla bone were fixed in 4% paraformaldehyde, decalcified in EDTA bone decalcifier, and then embedded in paraffin. These sections were prepared before hematoxylin and eosin (H&E) and immunohistochemical staining.

Statistical analysis

Statistical analyses were performed using SPSS 13.0 software

Table 2. Primer sequences for real-time PCR analysis on SD rat gingival.

Gene	Forward primer (5'–3')	Reverse primer (5'–3')
β-Actin SD rat	CCCATCTATGAGGGTTACGC	TTTAATGTCACGCACGATTTC
TNF-a SD rat	TCTTCTCATTCCTGCTCGTG	GAGGCTGACTTTCTCCTGGT
IL-1β SD rat	CTATGTCTTGCCCGTGGAG	CTGCTTGAGAGGTGCTGATG
IL-6 SD rat	CCACTGCCTTCCCTACTTCA	TCTTGGTCCTTAGCCACTCC

(SPSS Inc, Chicago, IL, USA). *P*-values were calculated by 2-tailed *t*-tests or one-way analyses of variance (grouped). *P*-values less than 0.05 were considered significant.

Results

Cytotoxicity of PL, OZ and TNF-α on PDLSCs

The cells were treated independently with different concentrations of PL (0–10 μmol/L), OZ (0–30 μg/mL) and TNF-α (0–30 ng/mL) for 24 h and 48 h. As shown in Figure 1, after 48 h of incubation, PL with a concentration of 10 μmol/L showed a significant cytotoxic effect on PDLSCs ($P<0.01$), which was not observed in the first 24 h. For OZ and TNF-α, no significant cytotoxic effects were observed at 24 h and 48 h in the tested concentration ranges.

PL inhibited the expressions of TNF-α, IL-1β and IL-6 in TNF-α-induced PDLSCs

Because TNF-α-induced inflammation results in the up-regulation of pro-inflammatory cytokines, such as TNF-α, IL-1β and IL-6, real-time PCR and ELISAs were conducted to evaluate the changes in expression levels of these cytokines. PDLSCs were treated with 10 ng/mL of TNF-α and different concentrations of PL (0–5 μmol/L) and OZ (0–10 μg/mL) for 24 h. Cells were collected for real-time PCR assays, and cell supernatants were collected for ELISAs. The gene expression levels of TNF-α, IL-1β and IL-6 increased with the induction of TNF-α and were down-regulated after treatment with PL, as shown in Figure 2. PL at 3.75 μmol/L had the greatest effect on decreasing all evaluated cytokines.

PL inhibited the expression of CCL-2 and CCL-5

Chemokines enhance the chemotaxis of macrophages, thereby accelerating the process of inflammation[25]. In our study, the expression levels of chemokines CCL-2 and CCL-5 were

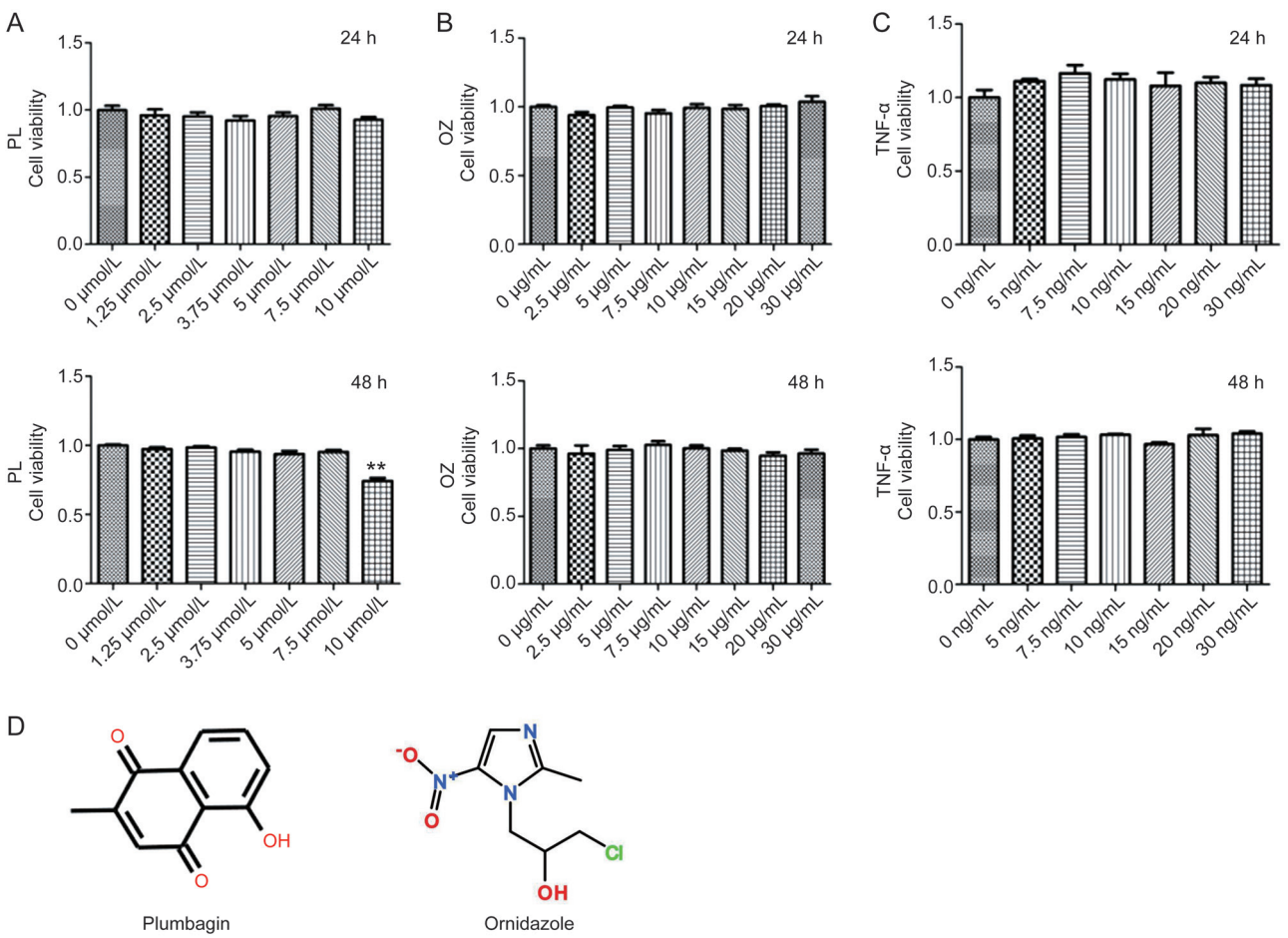

Figure 1. Cell viability of PDLSCs after individual treatment with PL (A), OZ (B) and TNF-α (C) for 24 h and 48 h. (D) Chemical structural formula of PL, OZ and TNF-α. The data are presented as the mean±SD. All experiments were repeated at least three times. $^{**}P<0.01$.

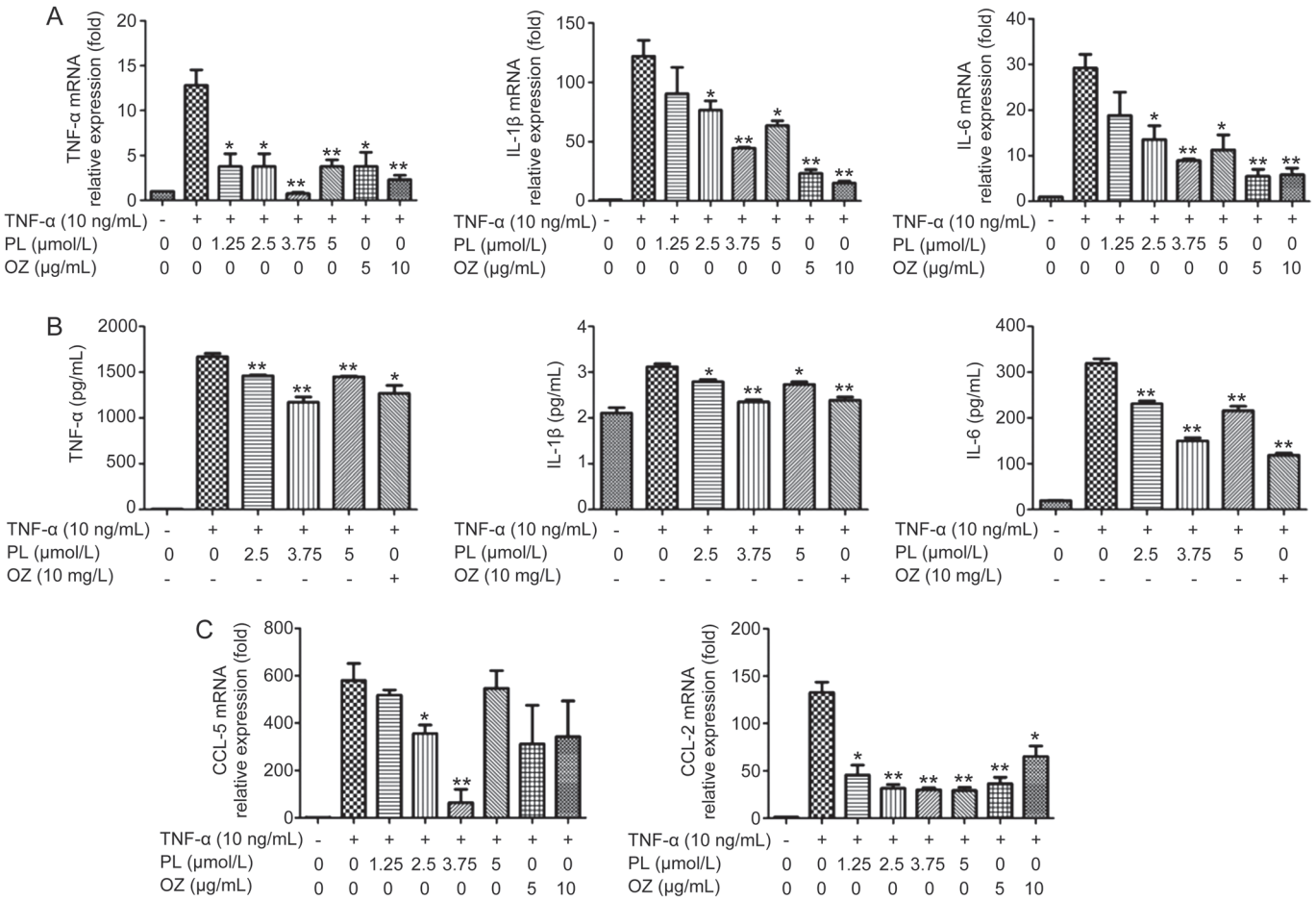

Figure 2. The effects of PL and OZ on the TNF-α-induced PDLSCs. (A) TNF-α, IL-1β and IL-6 mRNAs were subjected to real-time PCR analysis after 24 h. The expression levels were normalized to that of β-actin. (B) The levels of TNF-α, IL-1β and IL-6 in the medium were measured using an ELISA kit. (C) The expressions of CCL-5 and CCL-2 mRNA were measured by real-time RT-PCR. The data are presented as the mean±SD. $^{*}P<0.05$, $^{**}P<0.01$ *vs* the (TNF-α"+", PL"0", OZ"0") group. All data were obtained from at least three independent experiments.

down-regulated after treatment with PL (Figure 2). Similarly to the evaluations of TNF-α, IL-1β and IL-6, 3.75 μmol/L PL had the greatest effect.

PL suppressed TNF-α-induced inflammation by inhibiting the MAPK, NF-κB and JAK/STAT signaling phosphorylations in time- and dose-dependent manners

The MAPK signaling pathway is activated by TNF-α through the P38, ERK and JNK signaling pathways[26]. NF-κB is activated by TNF-α through p65. JAK/STAT signaling is activated by IL-6, which was upregulated by TNF-α stimulation (Figure 3)[27]. Western blotting results indicated that PL inhibited MAPK, NF-κB and JAK/STAT signaling phosphorylation in time- and dose-dependent manners (Figure 4 and 5). For the MAPK pathway, p-P38 was inhibited after 6 h ($P<0.01$), whereas p-ERK and p-JNK were inhibited after 2 h ($P<0.01$). For NF-κB signaling, p-P65 was inhibited after 4 h ($P<0.05$). p-STAT3 was also inhibited after 4 h ($P<0.01$). Western blotting of different concentrations of PL was also conducted, and all results showed that 3.75 μmol/L was the most effective dose for TNF-α-induced PDLSCs ($P<0.01$).

PL decreased bone destruction in ligation+Pg-stimulated animal models

Maxilla bones collected from SD rats were scanned and reconstructed to generate three-dimensional models. Alveolar bone loss (ABL), *ie*, the linear distance of CEJ to ABC, was measured at four points on each tooth (M1 and M2; Figure 6). ABL increased after ligation ($P<0.01$). The results indicated that 4 mg/kg PL had the most significant decrease in alveolar bone destruction ($P<0.01$ for M1 and overall, $P<0.01$ for M2), whereas all 3 different PL doses showed significant suppressive effects (2, 4, and 6 mg/kg).

Microstructure indicators of bone volume/tissue volume (BV/TV), trabecular thickness (Tb.Th), trabecular separation (Tb.Sp) and trabecular number (Tb.N) were measured (Figure 6). The results showed significance for only BV/TV and Tb.Th in the ligation and PL 4 mg/kg group, thus confirming the findings of a previous study by Xu that has found that ligation only slightly decreases maxilla bone mineral density (BMD)

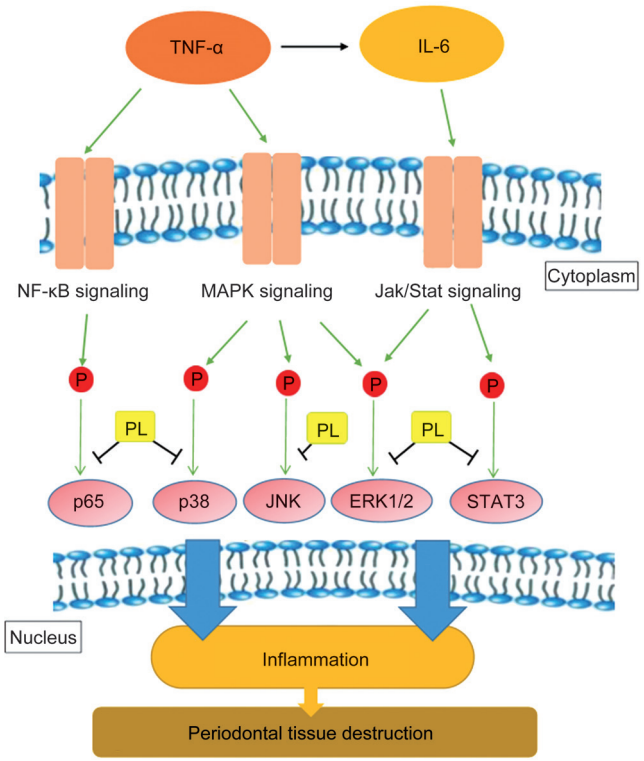

Figure 3. A schematic diagram of the proposed mechanisms on suppression effect of PL on chronic periodontitis via the inhibition of MAPK, NF-κB and JAK/STAT signaling pathways.

and bone formation rate but significantly enhances ABL[28]. H&E staining images showed widened periodontal membranes and descending alveolar bone crests in the ligation group (Figure 6). There was a significant decrease in periodontal membrane width and ABC in the PL-treated groups. PL at 4 mg/kg had the greatest effect.

PL promoted decreases in TNF-α, IL-1β and IL-6 in the animal model

Real-time PCR and immunohistochemical staining were performed to investigate the expression of relevant cytokines TNF-α, IL-1β and IL-6 in the SD rat model. The results of the real-time PCR on animal gingiva are shown in Figure 7. Increased mRNA expression was observed in the ligation groups compared with the control groups. TNF-α level was decreased after PL treatments of 2, 4, and 6 mg/kg (P<0.05). IL-1β level was decreased after PL treatments of 4 and 6 mg/kg (P<0.05). IL-6 level was decreased after PL treatments of 2 and 4 mg/kg (P<0.01 for 2 mg/kg, P<0.01 for 4 mg/kg).

The immunohistochemical staining analyses indicated that ligated SD rats had increased counts of TNF-α, IL-1β and IL-6 immunoreactive cells at periodontal ligament and alveolar sites. However, plumbagin-administered rats experienced decreases in TNF-α, IL-1β and IL-6, as reflected by the decreased quantity and darker appearance of the immunoreactive cells. The immunoreactive cells of TNF-α, IL-1β and IL-6 had brown-colored cytoplasm in immunohistochemical

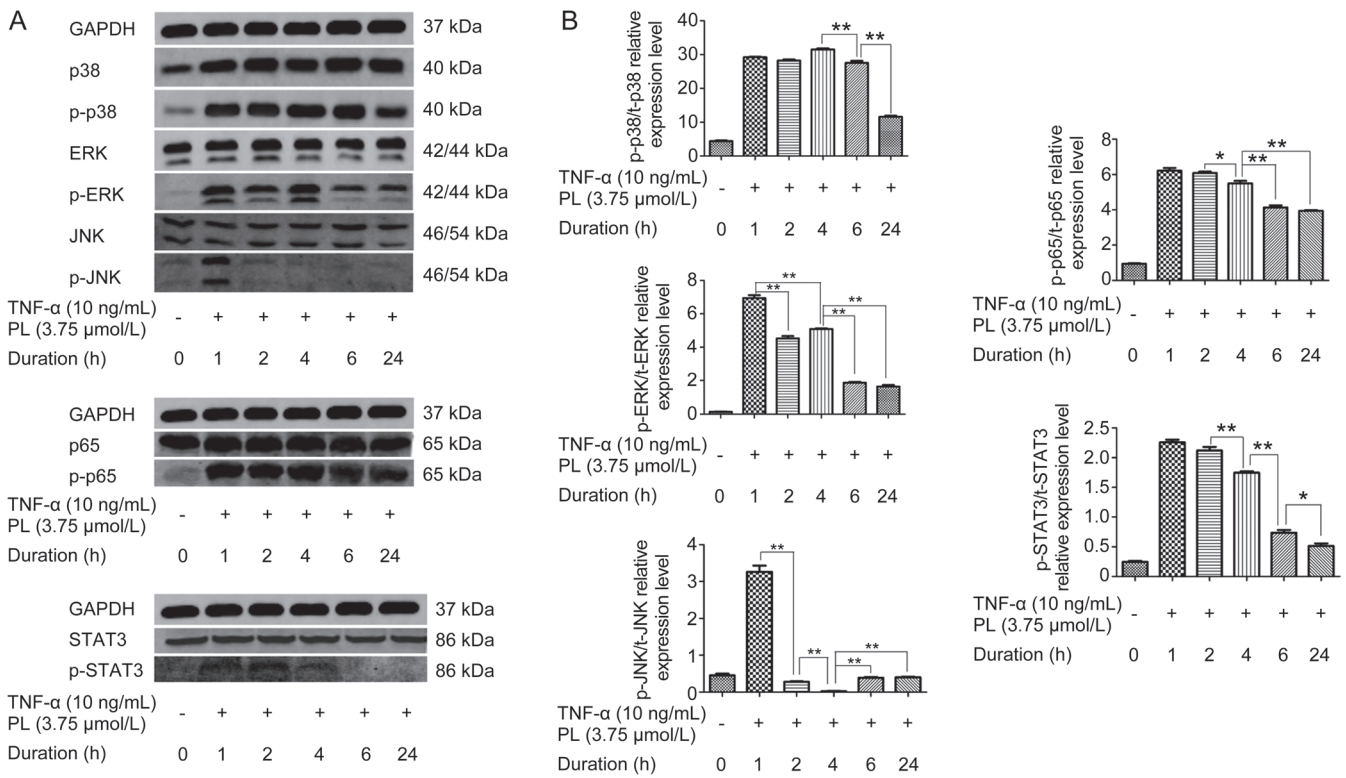

Figure 4. The effects of different duration of PL treatment on MAPK, NF-κB and JAK/STAT phosphorylation in TNF-α-induced PDLSCs. PL at a concentration of 3.75 μmol/L stimulated by 10 ng/mL TNF-α was cultured for 0, 1, 2, 4, 6 and 24 h. (A) The levels of p38, ERK, JNK, p65 and STAT3 and phosphorylated p38, ERK, JNK, p65 and STAT3 were examined in whole-cell lysates via Western blotting. (B) The relative expression levels of p-p38/p38, p-ERK/ERK, p-JNK/JNK, p-p65/p65 and p-STAT3/STAT3 were calculated based on the analysis of the gray band intensities. The data are presented as the mean±SD. $^{*}P$<0.05, $^{**}P$<0.01. All data were obtained from at least three independent experiments.

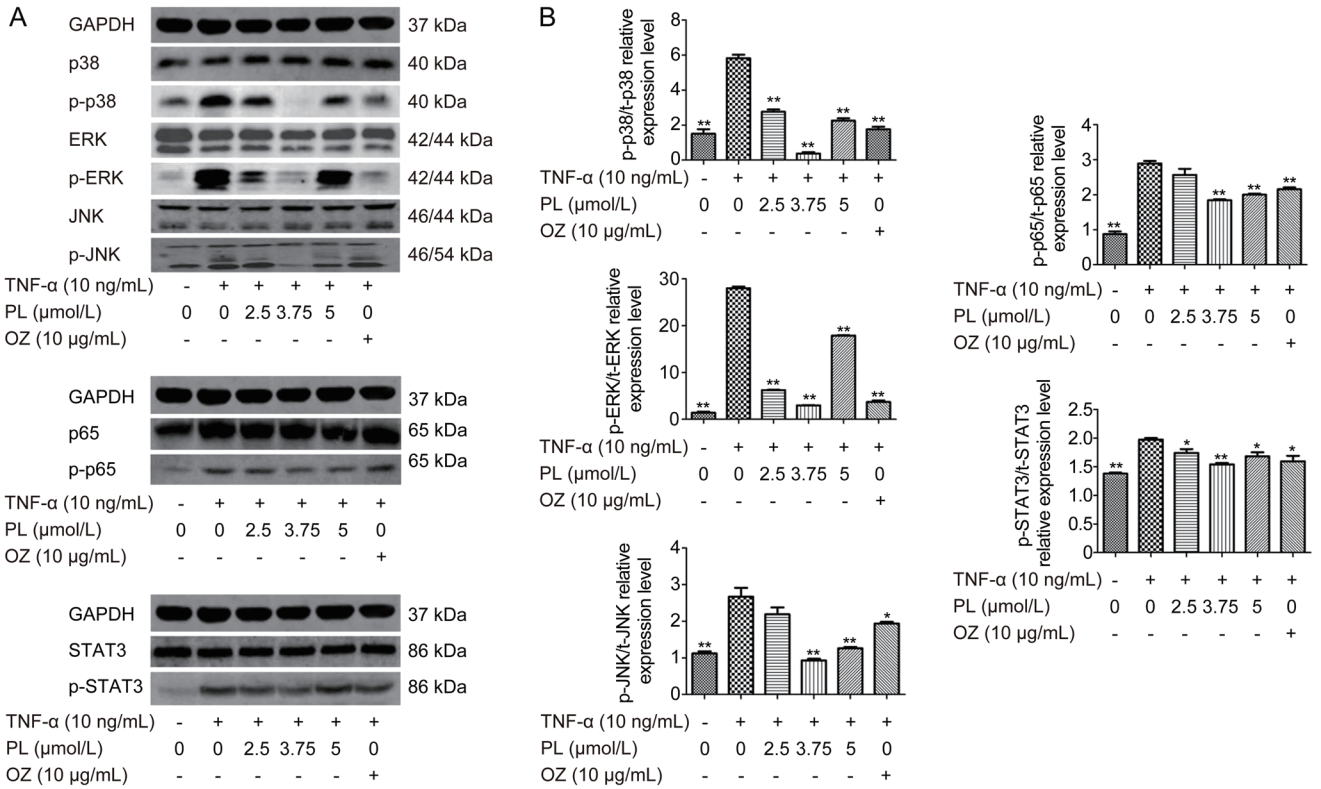

Figure 5. The effects of PL and OZ on MAPK, NF-κB and JAK/STAT phosphorylation in TNF-α-induced PDLSCs. The cells were treated with 10 ng/mL of TNF-α and different concentration of PL (0, 2.5, 3.75 and 5 μmol/L) and OZ (10 μg/mL) for 24 h. (A) The levels of P38, ERK, JNK, p65 and STAT3 and phosphorylated p38, ERK, JNK, p65 and STAT3 were examined in whole-cell lysates via Western blotting. (B) The relative expression levels of p-p38/p38, p-ERK/ERK, p-JNK/JNK, p-p65/p65 and p-STAT3/STAT3 were calculated based on the analysis of the gray band intensities. The data are presented as the mean±SD. $^{*}P<0.05$, $^{**}P<0.01$ *vs* the (TNF-α"+", PL"0", OZ"0") group. All data were obtained from at least three independent experiments.

staining. PL at 4 mg/kg showed the greatest effect in inhibiting inflammation (Figure 7).

Discussion

The levels of pro-inflammatory cytokines IL-1β and TNF-α increase during the pathogenesis of periodontitis[29,30]. Much of the damage that occurs during periodontal tissue destruction, such as attachment loss and alveolar bone loss, can be attributed to IL-1β and TNF-α activity. However, these cytokines also induce other mediators that act on the periodontal tissue, thereby accelerating the inflammatory response. The activation of inflammatory effects includes three pathways: the mitogen-activated protein kinase (MAPK) signaling pathway, the nuclear factor-kB (NF-κB) signaling pathway and the Janus tyrosine family kinase (JAK)-signal transducer and activator of transcription (STAT) (JAK/STAT) pathway.

MAPKs include p38 MAPK, c-Jun NH2-terminal kinase (JNK) and extracellular signal-regulated kinase (ERK)[31]. These enzymes are regulated by a characteristic phosphorylation system in which these enzymes activate one another. The JNK and p38 MAPK signaling pathways contribute to inflammation progression through activation by pro-inflammatory cytokines, such as tumor necrosis factor-α and interleukin 1β[32], whereas the Ras–Raf–MEK–ERK signaling pathway regulates proliferation and metastasis[33].

The nuclear factor-κB (NF-κB) pathway plays an important role in mediating inflammation. The phosphorylation of p65, which is targeted by various signaling pathways and protein, is enhanced by TNF-α and significantly inhibited by PL[34]. The binding of IL-6 to the IL-6-receptor leads to the activation of the following signaling pathways: the Janus tyrosine family kinase (JAK)-signal transducer and activator of transcription (STAT) pathway, the extracellular signal-regulated kinase 1 and 2 (ERK1/2)-mitogen-activated protein kinase (MAPK) pathway, and the phosphoinositide 3-kinase (PI3-K) pathway[35]. In our study, IL-6 was upregulated by TNF-α induction and activated ERK1/2 and STAT3 phosphorylation, thereby leading to enhanced inflammation.

Chronic periodontitis, caused by various oral organisms, is one of the main causes of tooth loss in adults[36]. These oral organisms affect oral conditions and lead to the progression of numerous systemic diseases, such as atherosclerosis, diabetes and pneumonia. Because the severity of CP is exacerbated with age, CP has a greater impact on the health of the elderly than the young[37]. The combination of mechanical and drug therapy, such as nitroimidazoles, has been the most effective

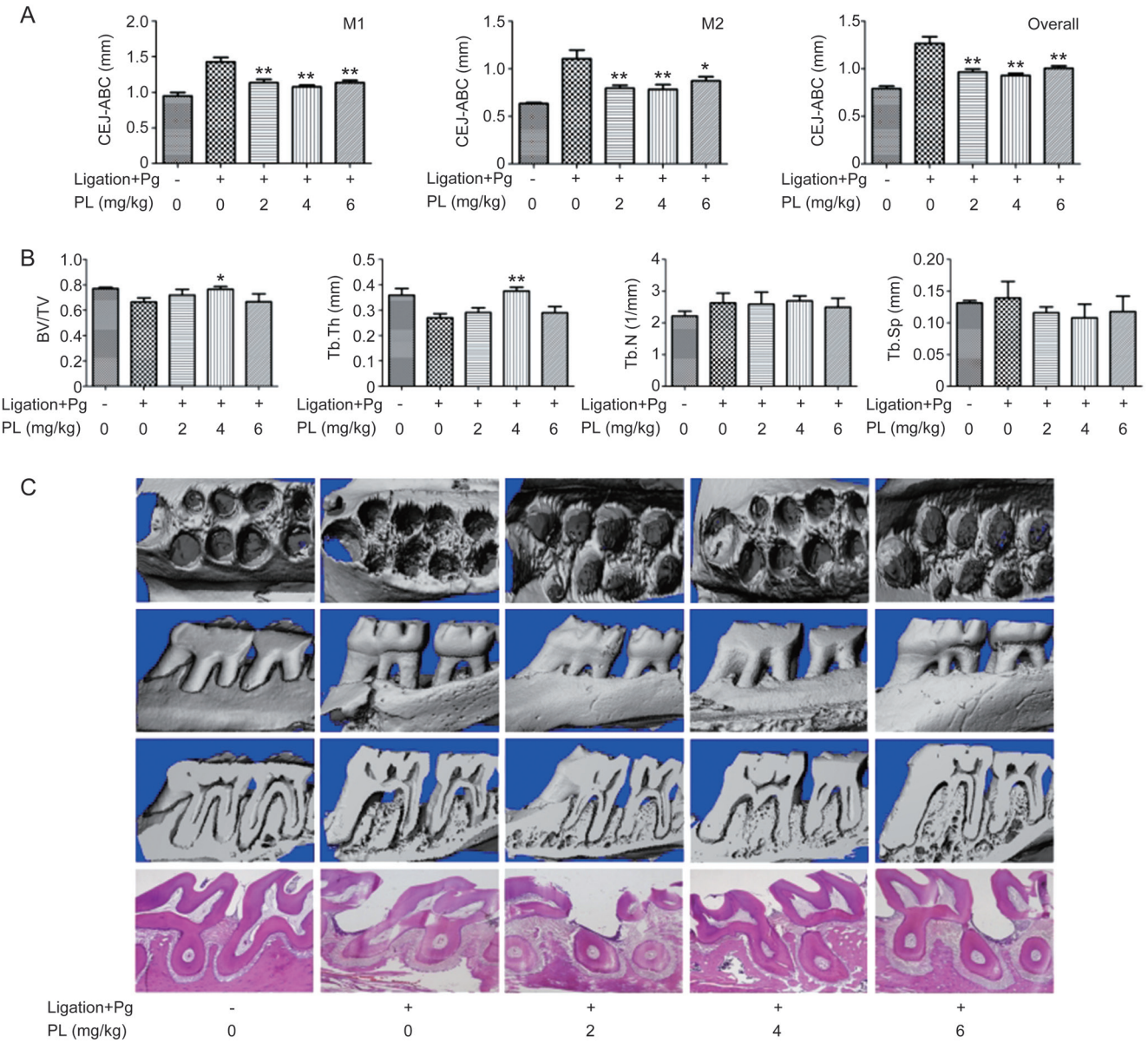

Figure 6. (A) Effect of PL on maxilla of cemento-enamel junction (CEJ) to alveolar bone crest (ABC). Buccal and palatal sides of the maxilla, where alveolar bone loss (ABL) was measured from the CEJ to the ABC at four points: mesiolingual (ML), mesiobuccal (MB), distolingual (DL), and distobuccal (DB) regions for first maxillary molar (M1) and second maxillary molar (M2). The overall result was also calculated. (B) Analysis of micro-CT volumetric parameters: bone volume/tissue volume (BV/TV), trabecular thickness (Tb.Th), trabecular number (Tb.N) and trabecular separation (Tb.Sp). (C) Descriptive analysis of micro-CT and H&E staining. The H&E staining images show sagittal sections of each group at 40× magnification. Values are expressed as the mean±SD. $^{*}P<0.05$, $^{**}P<0.01$ *vs* the (Ligation+Pg"+", PL"0") group.

treatment that leads to favorable healing[38]. Nitroimidazoles include metronidazole, ornidazole, and tinidazole. Among these, ornidazole has comparably better antibacterial properties than metronidazole and has fewer side effects. However, certain side effects still exist, such as gastric uneasiness, dizziness and antibiotic resistance[39]. Plumbagin is a traditional Chinese medicine extracted from plants. It has been used for centuries as an anti-inflammatory drug. The few reported side effects suggest its safety and superiority.

Most studies on the properties of PL have investigated the dose and duration of PL treatments. The results have varied, owing to different cells and diseases studied. Zhang *et al* have found that 10 μmol/L Plumbagin shows effective protection against dexamethasone-induced cell death in 24 h in osteoblastic MC3T3-E1 cells[12]. Han has found that 10 μmol/L PL exhibits a synergistic effect for all zoledronic acid concentrations examined in breast cancer cells, whereas 5 and 2.5 μmol/L shows significance after 48 h and 96 h[17]. Plumbagin exhibits high cytotoxicity against MG-63 human osteosarcoma cells with an IC_{50} of 15.9 μg/mL in 24 h[16]. Wang has reported

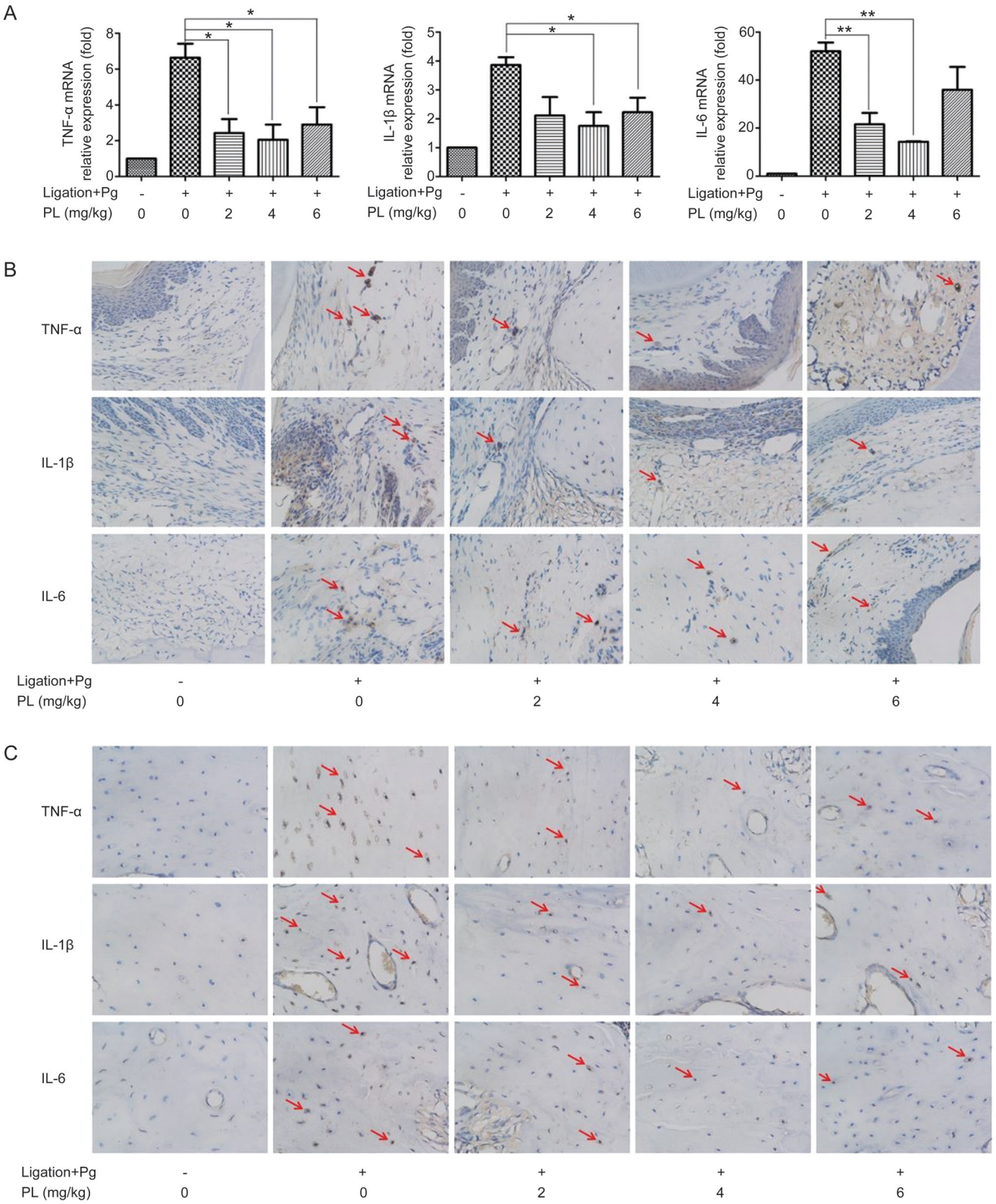

Figure 7. TNF-α, IL-1β and IL-6 expression levels in SD rat model. (A) Real-time PCR analysis was done on SD rat gingiva. The expression levels were normalized to that of β-actin. The data are presented as the mean±SD. $^{*}P<0.05$, $^{**}P<0.01$. (B) Immunohistochemical staining images on periodontal ligament sites at 400× magnification. (C) Immunohistochemical staining images on alveolar bone sites at 400× magnification. Arrows represent the immunoreactive cells.

that 2.5–7.5 μmol/L PL inhibits LPS-induced inflammation in RAW 264.7 cells in 48 h; the effect improves with increasing dose[15].

In animal experiments in this study, SD rats with intraperitoneal injections of 4 mg/kg PL for 4 weeks showed the greatest effects in decreasing periodontal destruction. In Chen's study on CCl_4-induced hepatic fibrosis, 3 mg/kg of PL twice a week for 4 weeks was intraperitoneally injected into SD rats[40]. Wang has administered C57BL6/J mice 5 mg/kg of PL by intraperitoneal injection for cardioprotection against myocardial I/R injury[14]. Hafeez has suggested that doses of 8 to 65 mg/kg body weight by oral administration and 16 mg/kg body weight by intraperitoneal administration in mice can inhibit prostate carcinogenesis, and has also observed that a 2000 ppm plumbagin diet is the maximum tolerated dose for mice[41]. In a study on Plumbagin inhibiting the invasion and migration of breast cancer, a dose of 4 mg/kg on BALB/c nude mice has proven effective[42].

In our study, PL was found to be effective at a relatively low dose and can decrease the risk of overdosage and drug toxicity.

We found that the type of drug administration has mostly been limited to intraperitoneal injections in past studies. Because drug therapy in treating chronic periodontitis can be classified as systemic and local therapy[43], the local administration of PL on CP should be further investigated.

This study provided an insight into PL for treatment of chronic periodontitis. In our study, we found that (i) PL inhibited the progression of inflammation by downregulating the expression of TNF-α, IL-1β and IL-6 through the MAPK, NF-κB and JAK/STAT signaling pathways in PDLSCs. (ii) Regarding reaction time, we examined the interaction of PL and TNF-α-induced PDLSCs from 0–24 h. Most of the signaling pathways were activated after 4 h, and the levels of inflammatory cytokines gradually increased. (iii) Decreases in the expression of CCL-2 and CCL-5 resulted in suppressed macrophage chemotaxis. (iv) Decelerated bone destruction, which is a sign of anti-inflammation, was observed in the ligation+Pg stimulation SD rat model, as indicated by ABL and H&E staining. (v) Decreases in TNF-α, IL-1β and IL-6 were observed in gingiva, periodontal ligament and alveolar bone area by real-time PCR and immunohistochemical staining, producing results consistent with the *in vitro* results.

Acknowledgements

This work was supported by grants from the National Natural Science Foundation of China (No 81570948), Science and Technology Commission of Shanghai Municipality (No 17140903400) and the Opening Project of Shanghai Key Laboratory of Orthopaedic Implant (No KFKT2015002).

Author contribution

Xin-yi ZHENG, Er-yi LU, Ting-yu WANG and Li YU designed research; Xin-yi ZHENG, Chuan-yuan MAO, Han QIAO and Xi ZHANG performed research; Ting-yu WANG and Li YU contributed new analytical tools and reagents; Xin-yi ZHENG and Chuan-yuan MAO analyzed data; Xin-yi ZHENG, Er-yi LU and Han QIAO wrote the paper.

References

1 Flemmig TF. Periodontitis. Ann Periodontol 1999; 4: 32–8.
2 Amano A. Bacterial adhesins to host components in periodontitis. Periodontol 2000 2010; 52: 12–37.
3 Liu R, Li N, Liu N, Zhou X, Dong ZM, Wen XJ, *et al*. Effects of systemic ornidazole, systemic and local compound ornidazole and pefloxacin mesylate on experimental periodontitis in rats. Med Sci Monit 2012; 18: 95–102.
4 Feres M, Figueiredo LC, Soares GM, Faveri M. Systemic antibiotics in the treatment of periodontitis. Periodontol 2000 2015; 67: 131–86.
5 Sekita Y, Murakami K, Yumoto H, Amoh T, Fujiwara N, Ogata S, *et al.* Preventive effects of *Houttuynia cordata* extract for oral infectious diseases. Biomed Res Int 2016; 2016: 2581876.
6 Wang Y, Zhang H, Du G, Wang Y, Cao T, Luo Q, *et al.* Total glucosides of paeony (TGP) inhibits the production of inflammatory cytokines in oral lichen planus by suppressing the NF-kappaB signaling pathway. Int Immunopharmacol 2016; 36: 67–72.
7 Inbaraj JJ, Chignell CF. Cytotoxic action of juglone and plumbagin: a mechanistic study using HaCaT keratinocytes. Chem Res Toxicol 2004; 17: 55–62.
8 Yan CH, Li F, Ma YC. Plumbagin shows anticancer activity in human osteosarcoma (MG-63) cells via the inhibition of S-Phase checkpoints and down-regulation of c-myc. Int J Clin Exp Med 2015; 8: 14432–9.
9 Padhye S, Dandawate P, Yusufi M, Ahmad A, Sarkar FH. Perspectives on medicinal properties of plumbagin and its analogs. Med Res Rev 2012; 32: 1131–58.
10 Luo P, Wong YF, Ge L, Zhang ZF, Liu Y, Liu L, *et al*. Anti-inflammatory and analgesic effect of plumbagin through inhibition of nuclear factor-kappaB activation. J Pharmacol Exp Ther 2010; 335: 735–42.
11 Chu H, Yu H, Ren D, Zhu K, Huang H. Plumbagin exerts protective effects in nucleus pulposus cells by attenuating hydrogen peroxide-induced oxidative stress, inflammation and apoptosis through NF-kappaB and Nrf-2. Int J Mol Med 2016; 37: 1669–76.
12 Zhang S, Li D, Yang JY, Yan TB. Plumbagin protects against glucocorticoid-induced osteoporosis through Nrf-2 pathway. Cell Stress Chaperones 2015; 20: 621–9.
13 Bhattacharya A, Jindal B, Singh P, Datta A, Panda D. Plumbagin inhibits cytokinesis in *Bacillus subtilis* by inhibiting FtsZ assembly-a mechanistic study of its antibacterial activity. FEBS J 2013; 280: 4585–99.
14 Wang SX, Wang J, Shao JB, Tang WN, Zhong JQ. Plumbagin mediates cardioprotection against myocardial ischemia/reperfusion injury through Nrf-2 signaling. Med Sci Monit 2016; 22: 1250–7.
15 Wang T, Wu F, Jin Z, Zhai Z, Wang Y, Ti B, *et al*. Plumbagin inhibits LPS-induced inflammation through the inactivation of the nuclear factor-kappa B and mitogen activated protein kinase signaling pathways in RAW 264.7 cells. Food Chem Toxicol 2014; 64: 177–83.
16 Yan W, Wang TY, Fan QM, Du L, Xu JK, Zhai ZJ, *et al*. Plumbagin attenuates cancer cell growth and osteoclast formation in the bone microenvironment of mice. Acta Pharmacol Sin 2014; 35: 124–34.
17 Qiao H, Wang TY, Yu ZF, Han XG, Liu XQ, Wang YG, *et al*. Structural simulation of adenosine phosphate via plumbagin and zoledronic acid competitively targets JNK/Erk to synergistically attenuate osteoclastogenesis in a breast cancer model. Cell Death Dis 2016; 7: e2094.
18 Lin J, Bi L, Yu X, Kawai T, Taubman MA, Shen B, *et al*. *Porphyromonas gingivalis* exacerbates ligature-induced, RANKL-dependent alveolar bone resorption via differential regulation of Toll-like receptor 2 (TLR2)

and TLR4. Infect Immun 2014; 82: 4127–34.
19 Górska R, Gregorek H, Kowalski J, Laskus-Perendyk A, Syczewska M, Madaliñski K. Relationship between clinical parameters and cytokine profiles in inflamed gingival tissue and serum samples from patients with chronic periodontitis. J Clin Periodontol 2003; 30: 1046–52.
20 Deo V, Bhongade ML. Pathogenesis of periodontitis: role of cytokines in host response. Dent Today 2010; 29: 60–2.
21 Sanz AR, Carrion FS, Chaparro AP. Mesenchymal stem cells from the oral cavity and their potential value in tissue engineering. Periodontol 2000 2015; 67: 251–67.
22 Zheng W, Wang S, Wang J, Jin F. Periodontitis promotes the proliferation and suppresses the differentiation potential of human periodontal ligament stem cells. Int J Mol Med 2015; 36: 915–22.
23 Park JC, Kim JM, Jung IH, Kim JC, Choi SH, Cho KS, *et al*. Isolation and characterization of human periodontal ligament (PDL) stem cells (PDLSCs) from the inflamed PDL tissue: *in vitro* and *in vivo* evaluations. J Clin Periodontol 2011; 38: 721–31.
24 Mao CY, Wang YG, Zhang , Zheng XY, Tang TT, Lu EY. Double-edged-sword effect of IL-1beta on the osteogenesis of periodontal ligament stem cells via crosstalk between the NF-kappaB, MAPK and BMP/Smad signaling pathways. Cell Death Dis 2016; 7: e2296.
25 Turner MD, Nedjai B, Hurst T, Pennington DJ. Cytokines and chemokines: at the crossroads of cell signalling and inflammatory disease. Biochim Biophys Acta 2014; 1843: 2563–82.
26 Kim EK, Choi EJ. Compromised MAPK signaling in human diseases: an update. Arch Toxicol 2015; 89: 867–82.
27 Ivanenkov YA, Balakin KV, Lavrovsky Y. Small molecule inhibitors of NF-kB and JAK/STAT signal transduction pathways as promising anti-inflammatory therapeutics. Mini Rev Med Chem 2011; 11: 55–78.
28 Xu XC, Chen H, Zhang X, Zhai ZJ, Liu XQ, Zheng XY, *et al*. Effects of oestrogen deficiency on the alveolar bone of rats with experimental periodontitis. Mol Med Rep 2015; 12: 3494–502.
29 Yucel-Lindberg T, Bage T. Inflammatory mediators in the pathogenesis of periodontitis. Expert Rev Mol Med 2013; 15: e7.
30 Graves DT, Cochran D. The contribution of interleukin-1 and tumor necrosis factor to periodontal tissue destruction. J Periodontol 2003; 74: 391–401.
31 Kim EK, Choi EJ. Compromised MAPK signaling in human diseases: an update. Arch Toxicol 2015; 89: 867–82.
32 Kirkwood KL, Rossa C Jr. The potential of p38 MAPK inhibitors to modulate periodontal infections. Curr Drug Metab 2009; 10: 55–67.
33 Chaikuad A, Tacconi EM, Zimmer J, Liang Y, Gray NS, Tarsounas M, *et al*. A unique inhibitor binding site in ERK1/2 is associated with slow binding kinetics. Nat Chem Biol 2014; 10: 853–60.
34 Chen X, Hu C, Wang G, Li L, Kong X, Ding Y, *et al*. Nuclear factor-kappaB modulates osteogenesis of periodontal ligament stem cells through competition with beta-catenin signaling in inflammatory microenvironments. Cell Death Dis 2013; 4: e510.
35 Nguyen DP, Li J, Tewari AK. Inflammation and prostate cancer: the role of interleukin 6 (IL-6). BJU Int 2014; 113: 986–92.
36 Reddy MS. Reaching a better understanding of non-oral disease and the implication of periodontal infections. Periodontol 2000 2007; 44: 9–14.
37 Scannapieco FA, Cantos A. Oral inflammation and infection, and chronic medical diseases: implications for the elderly. Periodontol 2000 2016; 72: 153–75.
38 Soskolne WA. Re: Impact of local adjuncts to scaling and root planing in periodontal disease therapy: a systematic review. Bonito AJ, Lux L, Lohr KN (2005;76:1227-1236). J Periodontol 2006; 77: 323–4.
39 Casagrande Tango R. Psychiatric side effects of medications prescribed in internal medicine. Dialogues Clin Neurosci 2003; 5: 155–65.
40 Chen S, Chen Y, Chen B, Cai YJ, Zou ZL, Wang JG, *et al*. Plumbagin ameliorates CCl_4-induced hepatic fibrosis in rats via the epidermal growth factor receptor signaling pathway. Evid Based Complement Alternat Med 2015; 2015: 645727.
41 Hafeez BB, Fischer JW, Singh A, Zhong W, Mustafa A, Meske L, *et al*. Plumbagin inhibits prostate carcinogenesis in intact and castrated PTEN knockout mice via targeting PKCα, Stat3, and epithelial-to-mesenchymal transition markers. Cancer Prev Res (Phila) 2015; 8: 375–86.
42 Yan W, Tu B, Liu YY, Wang TY, Qiao H, Zhai ZJ, *et al*. Suppressive effects of plumbagin on invasion and migration of breast cancer cells via the inhibition of STAT3 signaling and down-regulation of inflammatory cytokine expressions. Bone Res 2013; 1: 362–70.
43 Rodrigues RM, Gonçalves C, Souto R, Feres-Filho EJ, Uzeda M, Colombo AP. Antibiotic resistance profile of the subgingival microbiota following systemic or local tetracycline therapy. J Clin Periodontol 2004; 31: 420–7.